0.0124 ± 0.003, using negative thermal ionization techniques and fractionation correcting to a $^{194}Pt/^{195}Pt$ ratio of 0.9734 (*38*).
33. E. Anders and N. Grevesse, *Geochim. Cosmochim. Acta* **53**, 197 (1989).
34. M. P. Gorton, E. S. Schandl, A. J. Naldrett, *Ocean Drilling Project Scientific Results, Leg 140*, in press.
35. R. J. Walker *et al.*, *Geochim. Cosmochim. Acta* **58**, 4179 (1994); M. F. Horan, R. J. Walker, V. A. Fedorenko, G. K. Czamanske, *ibid.*, in press.
36. J.-M. Luck and C. J. Allègre, *Nature* **302**, 130 (1983).
37. J. W. Morgan, G. A. Wandless, R. K. Petrie, A. J. Irving, *Tectonophysics* **75**, 47 (1981).
38. P. De Bievre *et al.*, *J. Phys. Chem. Ref. Data* **13**, 809 (1984).
39. We thank R. Brett, B. Doe, S. Shirey, E. Widom, and two anonymous reviewers for reviewing preliminary versions of this manuscript. Supported by National Aeronautics and Space Administration grant NAGW 3625, NSF grant EAR 9117684, and the U.S. Geological Survey. We gratefully acknowledge this support.

13 March 1995; accepted 6 June 1995

High-³He Plume Origin and Temporal-Spatial Evolution of the Siberian Flood Basalts

Asish R. Basu,* Robert J. Poreda, Paul R. Renne, Friedrich Teichmann, Yurii R. Vasiliev, Nikolai V. Sobolev, Brent D. Turrin

An olivine nephelinite from the lower part of a thick alkalic ultrabasic and mafic sequence of volcanic rocks of the northeastern part of the Siberian flood basalt province (SFBP) yielded a $^{40}Ar/^{39}Ar$ plateau age of 253.3 ± 2.6 million years, distinctly older than the main tholeiitic pulse of the SFBP at 250.0 million years. Olivine phenocrysts of this rock showed $^{3}He/^{4}He$ ratios up to 12.7 times the atmospheric ratio; these values suggest a lower mantle plume origin. The neodymium and strontium isotopes, rare earth element concentration patterns, and cerium/lead ratios of the associated rocks were also consistent with their derivation from a near-chondritic, primitive plume. Geochemical data from the 250-million-year-old volcanic rocks higher up in the sequence indicate interaction of this high-³He SFBP plume with a suboceanic-type upper mantle beneath Siberia.

More than 20 years after Morgan (*1*) postulated the connections between continental flood basalt provinces (CFBPs), mantle plume activity, and continental rifting, there is now some general agreement on the role of deep mantle plumes in CFBP generation. Questions remain, however, regarding the nature of dispersal of the plume head in the upper mantle beneath the relatively cooler and rigid lithosphere, and the timing of melting initiated by the arrival of the hot plume at the base of the lithosphere is a topic of current investigations (*2–5*). In this report, we use $^{3}He/^{4}He$ as a diagnostic tracer to infer a lower mantle plume origin for the SFBP, the largest Phanerozoic CFBP; on the basis of combined isotopic and trace element characteristics, we also infer the involvement of an upper mantle component analogous to the present-day suboceanic mantle. We provide $^{40}Ar/^{39}Ar$ geochronologic data, He isotopic measurements, rare earth element (REE) data, and Sm-Nd and Rb-Sr isotope systematics data on a suite of alkalic ultrabasic and mafic volcanic rocks from the Maimecha-Kotui section of the SFBP. These data allow comparison with the flood basalts of the Deccan traps in India, which also contain high-³He rocks (*3*).

The SFBP erupted by mantle plume volcanism at the Permian-Triassic boundary (*6–13*). However, as with other flood basalt provinces, opinions vary concerning the relative amounts of magma contributed by crustal, subcontinental lithospheric, and upper and lower mantle sources (*14*). We attempted to resolve this issue by focusing on a suite of alkalic ultrabasic and basic rocks from the Maimecha-Kotui section (Fig. 1). These rocks make up about 2% of the SFBP by volume and are located northeast of the main Putorana sequence (Fig. 1). The Maimecha-Kotui suite of rocks forms a relatively thick series of alkaline, subalkaline, and ultrabasic rocks and includes different alkalic basalts, trachybasalts, trachyandesites, alkali trachytes, and rare maimechites (olivine-phyric picrites) (*15, 16*). This alkalic volcanic subprovince is located in an elongated region, presumably a graben, situated between the Tunguska basin to the west and the Anabar antiform to the east (*17*). The tectonic setting for these alkalic rocks is markedly different from that of the rest of the Siberian platform, which is covered by thick, monotonous tholeiites of the SFBP.

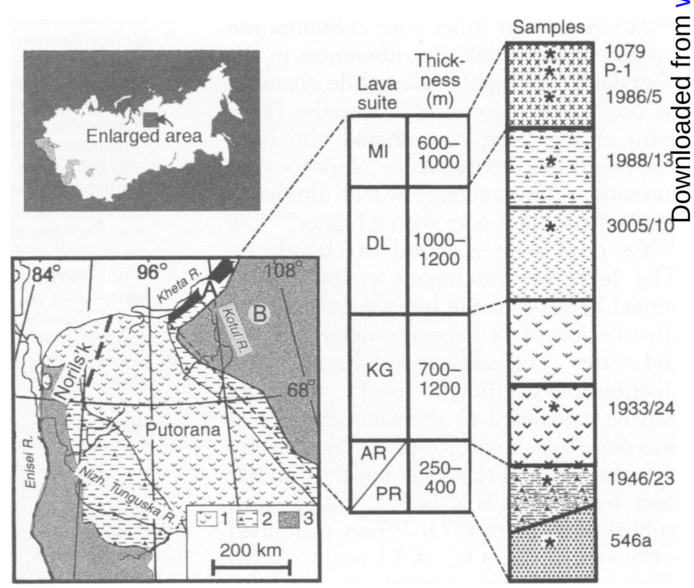

Fig. 1. Schematic geological map, on the left, of the Permian-Triassic volcanic rocks from the Siberian platform [modified after (*6*)] showing Norils'k, Putorana, and Maimecha-Kotui (in black), the three main sections of the SFBP. The Tertiary-Quaternary sediments are in white; other lithologies are 1, basalt trap; 2, intrusive trap and tuffs; and 3, platform sedimentary sequence. The thick dashed line represents the Norils'k-Putorana boundary. Two alkalic ultrabasic complexes are also shown: Gulin (A) and Odikhinca (B). The column on the right represents a composite volcano stratigraphy (*15*) of the Maimecha-Kotui section, with the relative locations of the samples analyzed in this study shown with asterisks. The lava suites and their approximate thicknesses are also shown in the middle two columns. The lava suites are as follows: Maimechinskay (MI), lavas, tuffs, and intrusive maimechites; Delkanskay (DL), lava flows of subalkaline basalts, trachybasalts, trachyandesites, andesites, shoshonites, and alkali picrites (upper sequence) and lava flows of augites, limburgites, nephelinites, analcitites, and tuffs (lower sequence); Kogotokskay (KG), subalkali basalts and trachybasalts (upper sequence) and tholeiitic and olivine basalts (lower sequence); and Aridgangskay (AR) and Pravobojrskay (PR), lava flows of augites, nephelinites, melilitites, picrites, tuffs, and olivine basalts.

A. R. Basu, R. J. Poreda, F. Teichmann, Department of Earth and Environmental Sciences, University of Rochester, Rochester, NY 14627, USA.
P. R. Renne, Berkeley Geochronology Center, 2455 Ridge Road, Berkeley, CA 94709–1211, USA.
Y. R. Vasiliev and N. V. Sobolev, Institute of Mineralogy and Petrology, Russian Academy of Sciences, Siberian Branch, Novosibirsk 630090, Russia.
B. D. Turrin, U.S. Geological Survey, Mailstop 901, 345 Middlefield Road, Menlo Park, CA 94025, USA, and Berkeley Geochronology Center, 2455 Ridge Road, Berkeley, CA 94709–1211, USA.

*To whom correspondence should be addressed.

We dated the olivine nephelinite (sample 1946/23) at the lower part of the Maimecha-Kotui section (Fig. 1) to determine the time of initiation of alkalic volcanism associated with the SFBP. Approximately 1 mg of plagioclase from this sample was prepared and analyzed by the incremental heating $^{40}Ar/^{39}Ar$ method (7, 18). Age calculations were based on an age of 28.03 ± 0.18 (2σ) Ma (million years ago) for Fish Canyon sanidine (19), which was used as a neutron fluence monitor. The apparent age spectrum (Fig. 2A) shows that the 12 steps together define a plateau age of 253.3 ± 4.0 Ma (2σ interlaboratory error, including the uncertainty in the age of the monitor). Neglecting uncertainty in the age of the monitor yielded an intralaboratory error of ±2.6 Ma. In a regression of $^{36}Ar/^{40}Ar$ versus $^{39}Ar/^{40}Ar$, the data defined an isochron with an age of 252.7 ± 3.1 Ma (2σ interlaboratory error), a mean squared weighted deviates (MSWD) value of 1.04, and an initial $^{40}Ar/^{36}Ar$ ratio of 296.4 ± 1.2 (indistinguishable from the present atmospheric value). The Ca/K spectrum (Fig. 2A, calculated from $^{37}Ar/^{39}Ar$) shows that this plagioclase is compositionally zoned in a normal sense, with more anorthitic cores outgassing at higher temperatures. Although its measurement is relatively imprecise because of the small sample size, low K content, and leverage of the Ca correction, the plateau age for sample 1946/23 is distinctly older than the age of the base of the Siberian traps near Norils'k. The beginning of main stage flood basalt volcanism reported by Renne and Basu (7), recalculated for the age of the monitor used here, is 250.0 ± 1.6 Ma (2σ interlaboratory error); because both samples were dated using the same fluence monitor, they can be compared solely on the basis of intralaboratory errors [±0.30 Ma for the sample in (7)]. Thus the plateau age of 253.3 ± 2.6 Ma in sample 1946/23 is clearly older than the initiation of main stage flood volcanism at 250.0 ± 0.3 Ma, and the predominantly alkalic volcanism of the Maimecha-Kotui section began distinctly before the main pulse of tholeiitic volcanism at Putorana and Norils'k. This situation is remarkably similar to that of Deccan flood volcanism, which also began with an early alkalic, isotopically primitive pulse 3 Ma before the main phase of tholeiitic volcanism (3).

We also dated a large single crystal of phlogopite associated with the pegmatoid olivinites of the Odikhinca intrusion (Fig. 1, location B). Apparent age spectra obtained by laser incremental heating of eight small wafers from various parts of the single crystal yielded variably discordant spectra, but all yielded indistinguishable plateau ages (Fig. 2B) ranging from 249.43 ± 0.50 to 250.43 ± 0.64 Ma. The weighted mean of these plateau ages is 249.88 ± 0.25 Ma (internal error; external error is ±1.53 Ma). The isochron age corresponding to the 84 plateau steps from all eight samples is 249.92 ± 1.63 Ma (external error), with a $^{40}Ar/^{36}Ar$ ratio of 294.7 ± 4.3 and a MSWD of 1.43. This age is identical to an age of 250.4 ± 1.3 Ma (when recalculated for the same fluence monitor age) that was recently reported (19) for a phlogopite from a maimechite flow associated with the Gulin intrusion (Fig. 1, location A), near the top of the stratigraphic column in Fig. 1. Thus, the termination of alkalic volcanism in the Maimecha-Kotui region was synchronous with the initiation of main stage tholeiitic volcanism of the SFBP to the southwest in Putorana and Norils'k (7).

We examined the isotopic composition and abundance of helium in olivine mineral separates from the olivine nephelinite (sample 1946/23) as well as from two maimechites (samples P-1 and 1079) from the top of the stratigraphic sequence (Fig. 1). The minerals, hand-picked clear grains, were crushed in several steps with progressively increasing duration and intensity un-

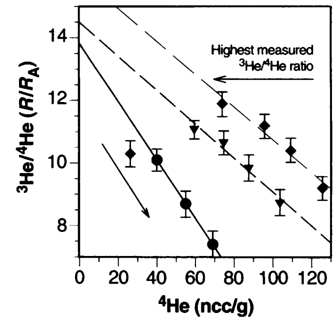

Fig. 3. The cumulative $^3He/^4He$ ratios, normalized to the atmospheric ratio (R_A), in each crushing step of olivine in sample 1946/23 are plotted against the ^4He concentrations. Different symbols represent the three different experimental measurements. The progressive decrease of $^3He/^4He$ as crushing proceeds (arrow at lower left) is indicative of the dominance of radiogenic ^4He and the absence of cosmogenic ^3He in the matrix, as also confirmed by a total fusion analysis [0.24R_A; 880 nano–cubic centimeters (ncc) of helium per gram].

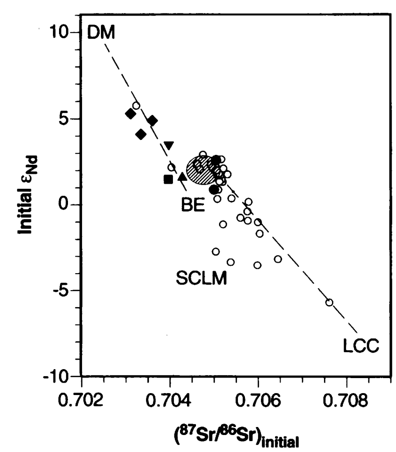

Fig. 4. Initial ϵ_{Nd} and $^{87}Sr/^{86}Sr$ ratios of eight Maimecha-Kotui samples (◆, maimechite; ■, olivine nephelinite; ●, olivine basalt; ▲, nepheline analcimite; ▼, trachybasalt) are compared with published results from the Putorana and Norils'k sections of the SFBP. The shaded region is the estimated bulk composition of the Siberian plume from an earlier study (10, 11). Results from several other studies (12), mostly on rocks from the Norils'k section, coincide with data points for basalts (○). DM, depleted mantle (MORB); BE, bulk chondritic earth; SCLM, subcontinental lithospheric mantle; and LCC, lower continental crust. The lower dashed line is a hypothetical mixing line between a "primitive" plume and LCC; some data points trend toward SCLM. An apparent mixing trend (upper dashed line) is defined by the Maimecha-Kotui rocks between the plume and the suboceanic upper mantle (DM).

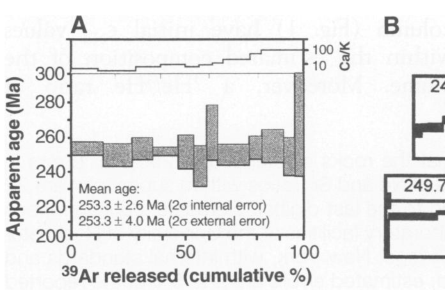

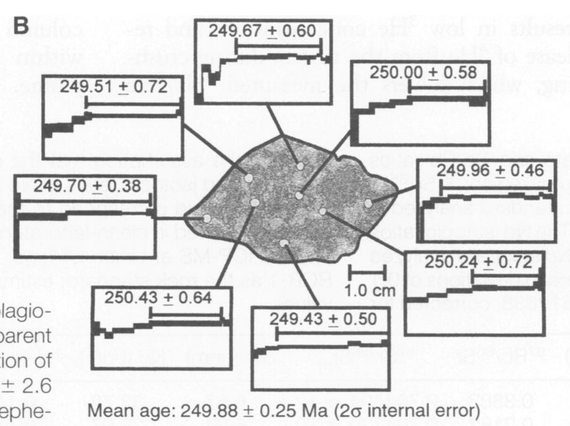

Fig. 2. (**A**) Apparent age spectrum of plagioclase in sample 1946/23 showing apparent age as a function of the cumulative fraction of ^{39}Ar released. The plateau age of 253.3 ± 2.6 Ma for the crystallization of this olivine nephelinite marks the first pulse of alkalic volcanism in the Maimecha-Kotui section; this age predates the main pulse of tholeiitic flood volcanism of the SFBP. (**B**) Apparent age spectra obtained by laser incremental heating of small wafers from a single crystal of phlogopite in olivinite of the Odikhinca intrusion (location B in Fig. 1). Plateaus are indicated and plateau ages for each are shown with 2σ internal uncertainties. The axes for each plot are the same as in (A). The plateau ages in (A) and (B) are based on the astronomically calibrated age of 28.03 ± 0.18 Ma for Fish Canyon sanidine (19).

Table 1. Helium isotopic ratios and noble gas abundances in the olivine separates from an olivine nephelinite and two maimechites from the Maimecha-Kotui section of the SFBP. Helium isotopic ratios, normalized to the ratio in air (R_A), were corrected for procedural blanks ($2 \pm 1R_A$; helium and neon abundances of 0.20 and 0.40 ncc, respectively) and air contribution, usually less than 1% for first-stage crushes.

Sample	Rock type	Weight of olivine (g)	Crushing		$^3He/^4He$ (R_A)	^4He (ncc/g)	^{22}Ne (ncc/g)	Cumulative	
			Step	Duration (min)				^4He (ncc/g)	$^3He/^4He$ (R_A)
1946/23 A	Olivine nephelinite	0.30	1	5	10.1 ± 0.2	40.0	0.11	40.0	10.1
			2	10	4.8 ± 0.1	14.9	0.13	54.9	8.7
			3	15	2.4 ± 0.05	14.1	0.16	69.0	7.4
1946/23 B	Olivine nephelinite	0.48	1	2	11.1 ± 0.2	59.0	0.23	59.0	11.1
			2	5	9.0 ± 0.2	14.9	0.14	73.9	10.7
			3	10	5.4 ± 0.1	13.0	0.16	86.9	9.9
			4	15	2.6 ± 0.05	15.7	0.15	102.6	8.8
1946/23 C	Olivine nephelinite	0.44	1	1	10.2 ± 0.2	26.9	0.15	26.9	10.2
			2	2	12.7 ± 0.2	48.4	0.18	75.3	11.8
			3	3	8.6 ± 0.2	21.8	0.21	97.1	11.1
			4	5	4.6 ± 0.1	13.5	0.18	110.6	10.3
			5	10	1.4 ± 0.03	15.3	0.18	125.9	9.2
1946/23 C	Powder	0.139	1	Until fusion	0.24 ± 0.05	880	0.73	—	—
P-1 A	Maimechite	0.98	1	5	4.4 ± 0.3	1.96	0.08	—	—
P-1 B	Maimechite	0.30	1	10	4.0 ± 0.4	1.33	0.10	—	—
1079 A	Maimechite	0.98	1	5	2.4 ± 0.2	2.04	0.08	—	—
1079 B	Maimechite	0.30	1	10	5.0 ± 0.6	1.22	0.12	—	—

der high vacuum to release the gases from the inclusions. These experiments were repeated several times (three times for sample 1946/23, twice each for samples P-1 and 1079; Table 1) on different mineral fractions from the same rock, with the use of experimental and analytical procedures given in (*20*). For sample 1946/23, the cumulative $^3He/^4He$ ratios are plotted against the ^4He concentrations in Fig. 3 for all three experimental measurements. Table 1 and Fig. 3 show that the $^3He/^4He$ ratio decreased in sample 1946/23 as crushing proceeded, which clearly indicates the addition of ^4He from the matrix and the absence of cosmogenic ^3He. We also confirmed this observation by measuring the radiogenic $^3He/^4He$ ratio in the fused olivine powder (Table 1). The highest measured $^3He/^4He$ ratio in step 2 of sample 1946/23 C in Table 1 is $12.7 \pm 0.2R_A$, where R_A is the atmospheric $^3He/^4He$ ratio. This ratio of $12.7R_A$ should be considered as a minimum value for the mantle source of the SFBP because the diffusion of radiogenic ^4He present in the matrix into the vapor inclusions would have reduced the $^3He/^4He$ ratio of this olivine from its crystallization ratio at 253 Ma. Because the matrix helium is dominantly radiogenic ^4He and not cosmogenic ^3He, there is no reasonable scenario that would assign the ^3He to anything other than a mantle source (*21*). Our data clearly demonstrate the usefulness of He isotopes as tracers for rocks at least as old as 253 Ma. The two maimechites (samples P-1 and 1079) in Table 1 show low abundances of ^4He as well as lower $^3He/^4He$ ratios in the olivines. The low $^3He/^4He$ ratio results from a combination of two processes: degassing of the melt before olivine formation, which results in low ^3He concentration, and release of ^4He from the matrix during crushing, which lowers the measured $^3He/^4He$ ratio. The $^3He/^4He$ ratios of samples P-1 and 1079 are not diagnostic of mantle sources.

The concentrations of Rb, Sr, Sm, and Nd and the isotopic compositions of Sr and Nd for eight volcanic rocks (Fig. 1) were determined along with their Ce/Pb ratios (Table 2). The initial isotopic ratios of Sr and Nd of these rocks are compared in Fig. 4 with previous results from the Norils'k and Putorana sections (*10–12*), which represent more than 95% of the SFBP. Sharma *et al.* (*11*) estimated an initial Nd isotopic ratio (ϵ_{Nd}) of $+1.8 \pm 0.7$ for the Siberian plume on the basis of samples from the voluminous, relatively uncontaminated lava of the Putorana section (Fig. 4, shaded region). The four samples from the lower part of the Maimecha-Kotui stratigraphic column (Fig. 1) have initial ϵ_{Nd} values within the estimated composition of the plume. Moreover, a $^3He/^4He$ ratio of

Table 2. Rb-Sr and Sm-Nd isotope systematics data and Ce/Pb ratios of eight whole-rock samples from the Maimecha-Kotui region; $^{87}Sr/^{86}Sr$ is normalized to $^{86}Sr/^{88}Sr = 0.1194$ [the NBS 987 Sr standard analyzed in our laboratory gave $^{87}Sr/^{86}Sr = 0.710243 \pm 20$ (2σ)]. The Nd isotopic ratios are normalized to $^{146}Nd/^{144}Nd = 0.7219$ [the La Jolla Nd standard analyzed during this study gave 0.511859 ± 18 (2σ)]; $\epsilon_{Nd}(T)$ refers to deviations of 0.1 per mil from the bulk-earth value of $^{143}Nd/^{144}Nd = 0.512638$, corrected for age with the assumption that the rocks crystallized at 250 Ma. Errors in the measured isotopic ratios of Nd and Sr (ratios with m subscripts) are 2σ of the mean and correspond to the last digit(s). Elemental concentrations were determined in clean-laboratory facilities at the University of Rochester and the ICP-MS at Union College, New York, with internal standards and BCR-1 as the rock standard; estimated errors are 2 to 5% of the reported values.

Sample	Rock type	Rb (ppm)	Sr (ppm)	$^{87}Rb/^{86}Sr$	$^{87}Sr/^{86}Sr_m$	Sm (ppm)	Nd (ppm)	$^{147}Sm/^{144}Nd$	$^{143}Nd/^{144}Nd_m$	$\epsilon_{Nd}(T)$	Ce/Pb
1079	Maimechite	59.67	442.4	0.3883	0.704494 ± 12	6.67	33.79	0.1194	0.512784 ± 10	5.3	33.5
P-1	Maimechite	25.81	340.3	0.2183	0.704120 ± 10	5.24	28.07	0.1129	0.512711 ± 6	4.1	31.3
1986/5	Maimechite	3.49	203.6	0.0493	0.703775 ± 29	3.19	17.01	0.1135	0.512750 ± 12	4.9	31.4
1988/13	Trachybasalt	53.54	1540.4	0.1000	0.704327 ± 13	23.82	143.80	0.1122	0.512659 ± 16	3.5	34.2
3005/10	Nepheline analcimite	54.93	1761.9	0.0897	0.704598 ± 31	18.56	122.67	0.0915	0.512546 ± 11	1.6	26.0
1933/24	Olivine basalt	2.20	173.7	0.0365	0.705121 ± 15	3.34	11.42	0.1770	0.512655 ± 10	1.0	10.6
1946/23	Olivine nephelinite	48.6	1441.2	0.0970	0.704306 ± 25	12.34	84.50	0.0884	0.512539 ± 10	1.5	29.0
546a	Olivine basalt	3.04	199.1	0.0440	0.705207 ± 17	3.55	12.63	0.1701	0.512727 ± 12	2.6	14.0

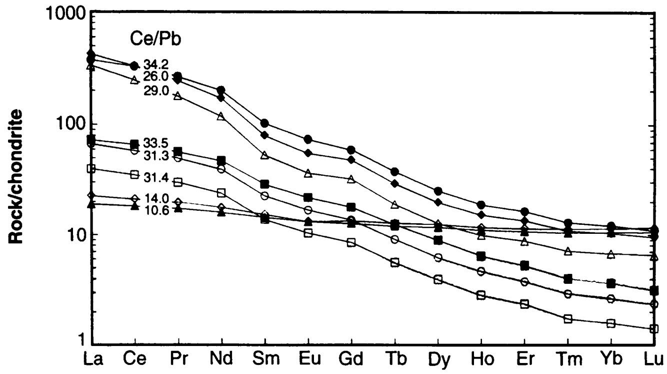

Fig. 5. REE concentrations, normalized to chondritic abundances, of eight volcanic rocks from the Maimecha-Kotui section (●, 1988/13; ◆, 3005/10; △, 1946/23; ■, 1079; ○, P-1; □, 1986/5; ◇, 546a; and ▲, 1933/24) are shown with their Ce/Pb ratios. The relatively flat patterns of the two olivine basalts also show near-chondritic Ce/Pb ratios of 10 and 14. The other rocks have Ce/Pb ratios typical of suboceanic mantle and show light-REE–enriched patterns.

$12.7R_A$ in sample 1946/23, which is presumably characteristic of lower mantle helium, is consistent with this observation. In contrast, the four samples from the top of the column, including the three maimechites, fall away from the lower samples toward the depleted mantle mid-ocean ridge basalt (MORB) component (Fig. 4). We interpret this negative correlation to indicate a mixing relation between the Siberian plume component (with a high $^3He/^4He$ ratio) and a suboceanic mantle reservoir in the generation of the upper-sequence volcanic rocks, particularly the maimechites. Thus, the early phase of Siberian flood basalt volcanism in the Maimecha-Kotui section reflects mixing between a plume and the depleted asthenosphere, whereas the final outburst of tholeiitic flood basalt volcanism in the Putorana and Norils'k sections indicates plume–continental lithospheric interactions, as reflected by their Nd-Sr mixing arrays (Fig. 4).

The above conclusions regarding the involvement of a lower mantle–derived plume with a suboceanic mantle in the early phase of SFBP are also supported by the REE data and the Ce/Pb ratios of the Maimecha-Kotui rocks (Fig. 5). These elements were analyzed by an inductively coupled plasma mass spectrometer (ICP-MS). Two undersaturated olivine tholeiites (with normative olivine and hypersthene) from the lower part of the column in Fig. 1 show characteristic flat REE patterns with small light-REE enrichments (Fig. 5). The Ce/Pb ratios of 10 to 14 for these rocks (Fig. 5 and Table 2) are close to 9, the estimated primitive mantle ratio (*22*), and are different from the relatively uniform upper mantle and continental crustal values of 25 ± 5 and 4, respectively. The Nd and Sr isotopic ratios of these basalts, as discussed above, are also within the estimated (*11*) SFBP plume composition, near the chondritic bulk-earth values (Fig. 4). The high-^3He–bearing olivine nephelinite and the higher level maimechites, however, show fractionated light-REE enrichment and Ce/Pb ratios of 29.0 to 33.5; these findings imply entrainment of some less primitive, suboceanic upper-mantle material by the lower mantle–derived plume. Thus, we conclude that the maimechites of Maimecha-Kotui are the results of late partial melting in a shallower mantle region of the evolving and ascending SFBP plume, either before or synchronous with the main stage of tholeiitic flood basalt volcanism in the Putorana region. Our results establish the significance of the relation between peripheral alkali magmatism and the voluminous tholeiites of the SFBP in the context of geodynamic and geochemical processes involving a high-^3He plume. The results also show that the exact timing and the tectonic setting of preflood volcanism compared to the flood basalts are critical to the interpretation of the chemical and isotopic data of the plume-generated SFBP.

REFERENCES AND NOTES

1. W. J. Morgan, *Nature* **230**, 42 (1971); *Bull. Am. Assoc. Petrol. Geol.* **56**, 203 (1972); in *The Sea*, C. Emiliani, Ed. (Wiley, New York, 1981), pp. 443–487.
2. R. A. Duncan and D. G. Pyle, *Nature* **333**, 841 (1988); M. A. Richards *et al.*, *Science* **246**, 103 (1989); R. G. Griffiths and I. H. Campbell, *Earth Planet. Sci. Lett.* **99**, 66 (1990); R. A. Duncan and M. A. Richards, *Rev. Geophys.* **29**, 31 (1991); R. W. Kent *et al.*, *Geology* **20**, 891 (1992).
3. A. R. Basu *et al.*, *Science* **261**, 902 (1993).
4. N. Sleep, *J. Geophys. Res.* **95**, 6715 (1990); J.-G. Schilling, *Nature* **352**, 397 (1991).
5. R. S. White and D. P. McKenzie, *J. Geophys. Res.* **94**, 7685 (1989).
6. V. V. Zolotukhin and A. I. Al'mukhamedov, in *Continental Flood Basalts*, J. D. Macdougall, Ed. (Kluwer, Dordrecht, Netherlands, 1988), pp. 273–310; G. I. Sadovnikov, *Izv. Akad. Nauk SSSR Ser. Geol.* **9**, 49 (1981).
7. P. R. Renne and A. R. Basu, *Science* **253**, 176 (1991).
8. I. H. Campbell *et al.*, *ibid.* **258**, 1760 (1992).
9. G. B. Dalrymple *et al.*, *Geochim. Cosmochim. Acta* **59**, 2071 (1995).
10. M. Sharma, A. R. Basu, G. V. Nesterenko, *Geochim. Cosmochim. Acta* **55**, 1183 (1991).
11. ———, *Earth Planet. Sci. Lett.* **113**, 365 (1992).
12. D. J. DePaolo and G. J. Wasserburg, *Proc. Natl. Acad. Sci. U.S.A.* **76**, 3056 (1979); P. C. Lightfoot *et al.*, *Contrib. Mineral. Petrol.* **114**, 171 (1993); J. L. Wooden *et al.*, *Geochim. Cosmochim. Acta* **57**, 3677 (1993).
13. P. R. Renne *et al.*, *Science*, in press.
14. R. W. Carlson *et al.*, *Geochim. Cosmochim. Acta* **47**, 845 (1983); D. J. DePaolo, *ibid.*, p. 841; J. J. Mahoney, in *Continental Flood Basalts*, J. D. Macdougall, Ed. (Kluwer, Dordrecht, Netherlands, 1988), pp. 151–194.
15. This column is based on unpublished field data compiled by Y. R. Vasiliev and co-workers.
16. Maimechite is an exclusive rock in this type locality in Siberia, where it is closely associated with ultrabasic rocks (dunites and peridotites) and alkalic rocks (picrites, nepheline picrites, olivine melanephelinites and nephelinites, and their extrusive equivalents). The maimechites are a late extrusive rock near the top of the sequence of lavas of the Maimecha-Kotui section (Fig. 1). They also occur as part of volcanic complexes that intrude the lava sequence. The typical maimechite is a coarsely porphyritic, ultrabasic rock with phenocrysts of olivine (50 to 70% by volume) and chrome spinel (1% by volume) in a groundmass consisting of olivine, clinopyroxene, titanomagnetite, phlogopite, and glass [A. V. Sobolev and A. B. Stutskii, *Geol. Geofiz.* **25**, 97 (1984)].
17. E. L. Butakova, in *The Alkaline Rocks*, H. Sorensen, Ed. (Wiley, New York, 1974), pp. 172–189. A small ocean basin between the Enisei and Ob rivers in West Siberia (Fig. 1), known as the Obsky paleoocean, has been confirmed by recent seismic, gravity, bore-hole, and magnetic data [S. Aplonov, *Tectonics* **7**, 1103 (1988)]; the identification of this north-south–trending buried spreading center along the axial zone of West Siberia and its correlation with the Paleozoic-Mesozoic boundary has important implications for the plume origin of the SFBP.
18. P. R. Renne *et al.*, *Science* **258**, 975 (1992).
19. P. R. Renne *et al.*, *Geology* **22**, 783 (1994).
20. R. J. Poreda and K. Farley, *Earth Planet. Sci. Lett.* **113**, 129 (1992).
21. We recognize that surface exposures can result in significant production of ^3He [H. Craig and R. J. Poreda, *Proc. Natl. Acad. Sci. U.S.A.* **83**, 1970 (1986); M. D. Kurz, *Nature* **320**, 435 (1986)] and that the decay of U and Th can generate both ^4He and ^3He by neutron interactions with Li and B. Although our stepwise crushing and fusion experiments (Table 1 and Fig. 3) clearly document that cosmogenic ^3He is relatively unimportant here, some qualitative estimates can also be made of the nucleogenic production of ^3He in 253 Ma. Under the assumption that the fluid inclusions (<1% by volume) in olivine have B and Li concentrations similar to alkalic magmas, the measured amounts of U (2.66 ppm) and Th (11.88 ppm) of the whole-rock sample 1946/23 could produce enough neutrons to react with the Li and B of the fluid inclusions to make ^3He. However, the amount of this nucleogenic ^3He produced in 253 Ma is less than 10% of the amount measured by crushing, and in all cases the nucleogenic He has a $^3He/^4He$ ratio lower than air. Another conceivable but improbable scenario would generate the ^3He by cosmogenic production and subsequent diffusion into the inclusions. For this situation, a surface exposure time of 250,000 years for the olivine nephelinite flow is needed immediately after extrusion so as to leave no trace of ^3He in the olivine matrix. However, sample 1946/23 occurs at a depth of >1 m below the surface of the flow, where the ^3He production is ≤1% of that at the surface. Therefore, the posteruptive He production is not at all detrimental to our argument that we have indeed measured the magmatic helium signature. The olivine separates of sample 1946/23 are not xenocrysts, as they appear as clear euhedral crystals. The olivines are 0.5 to 3 mm in size and they contain up to 0.8% fluid inclusions by volume. The composition of this olivine is $(Mg_2SiO_4)_{82}(Fe_2SiO_4)_{18}$, similar to olivine phenocrysts commonly crystallizing from basaltic melts and grossly different from mantle peridotite-derived, xenocrystic olivine found in alkalic basalts.
22. A. W. Hofmann, K. P. Jochum, M. Seufert, W. M. White, *Earth Planet. Sci. Lett.* **79**, 33 (1986).

23. Partially supported by NSF, the Berkeley Geochronology Center, and the Siberian Branch of the Russian Academy of Sciences. We are grateful to A. Sobolev for providing two samples of maimechites and for helpful discussions on the petrology and geochemistry of these rocks. We thank R. Hannigan for help with the illustrations.

31 March 1995; accepted 20 June 1995